Solution to the unknown boundary tractions in myocardial material parameter estimations

Anastasia Nasopoulou[1] (✉), David A. Nordsletten[1,2], Steven A. Niederer[1], and Pablo Lamata[1]

1. Department of Biomedical Engineering, Division of Imaging Sciences and Biomedical Engineering, King's College London, London, UK
2. Department of Biomedical Engineering and Cardiac Surgery, University of Michigan, Ann Arbor MI, USA
anastasia.nasopoulou@kcl.ac.uk

Abstract. Passive material parameter estimation can facilitate the in vivo assessment of myocardial stiffness, an important biomarker for heart failure stratification and screening. Parameter estimation strategies employing biomechanical models of various degrees of complexity have been proposed, usually involving a significant number of cardiac mechanics simulations. The clinical translation of these strategies however is limited by the associated computational cost and the model simplifications. A simpler and arguably more robust alternative is the use of data-based approaches, which do not involve mechanical simulations and can be based for example on the formulation of the energy balance in the myocardium from imaging and pressure data. This approach however requires the estimation of the mechanical work at the myocardial boundaries and the strain energy stored, tasks that are challenging when external loads are unknown - especially at the base which deforms extensively within the cardiac cycle. In this work we employ the principle of virtual work in a strictly data-based approach to uniquely identify myocardial material parameters by eliminating the effect of the unknown boundary tractions at the base. The feasibility of the method is demonstrated on a synthetic data set using a popular transversely isotropic material model followed by a sensitivity analysis to modelling assumptions and data noise.

1 Introduction

It is a known hypothesis that myocardial remodelling occurring in cardiac disease may result in changes in myocardial tissue stiffness. Recently stiffness was identified as a powerful biomarker for the diagnosis and monitoring of heart failure (HF) with preserved ejection fraction, a syndrome affecting 50% of HF patients [11]. Stiffness estimation however is not directly available in vivo and for this reason biomechanical models are used to identify the material parameters that best match model predictions to data observations.

Most of the available parameter estimation pipelines are based on the comparison between data (usually deformations) and model predictions. As such,

these methods require the execution of many mechanical simulations and/or nonlinear optimisation routines, which are accompanied by a significant computational burden. Moreover, there is a limited overlap between the space of deformations in actual data and those reproduced by mechanical simulations, caused by the presence of data artefacts and a series of model assumptions [10, 6].

There is thus a need to progress towards real-time and accurate myocardial tissue stiffness estimation for translation to the clinic. Data based approaches in parameter estimation are a valid candidate to achieve this goal, since they do not require to run simulations. Instead, they propose a physical interpretation of the deformation and pressure data, based for example on energetics analysis. Arguably, the expression of energy conservation can provide a richer metric in terms of information than the point by point comparison of a distance or strain based metric, especially in the context of material parameter estimation. And it has been shown to solve the lack of identifiability of material parameters of the myocardium [9, 8], thus having the potential of rendering a more accurate parameter estimation pipeline for diagnostic and prognostic purposes. One of the limitations of this approach is that it requires the estimation of the work at the myocardial boundaries and the strain energy stored, tasks that are challenging when external loads are unknown, especially at the base which deforms extensively within the cardiac cycle.

In this work we employ the principle of virtual work in a strictly data-based approach (parameter estimation is based on data analysis without the need for mechanical simulations) to eliminate the effect of the unknown boundary tractions while keeping the advantage of uniquely identifying myocardial material parameters. We thus take a closer look into the energetics analysis of the myocardium, quantify the impact associated with the unaccounted boundary tractions at the base and identify a virtual deformation field that can be used to remove their impact from the parameter identification task.

2 Materials and Methods

2.1 Material model

The myocardium in this study was modelled according to the transversely isotropic model introduced by Guccione et al. [3]. Here we use a modified formulation of this expression proposed by Xi et al. [12], focusing on the scaling parameter C_1 and the bulk exponential parameter α (Eq. (1)). The parameters r_f,r_t,r_{ft} scale the Green-Lagrange strain tensor ($\boldsymbol{E}$) components along the fiber direction (f), in the transverse plane (t) and in the fiber-transverse shear plane and $\boldsymbol{E}$ is expressed in the local fiber coordinate system where f,s,n denote the fiber, sheet and sheet normal directions.

$$\begin{aligned} \Psi &= \frac{1}{2}C_1(\mathrm{e}^Q - 1) \\ Q &= \alpha[r_f {E_{ff}}^2 + r_{ft}(2{E_{fs}}^2 + 2{E_{fn}}^2) + r_t({E_{ss}}^2 + {E_{nn}}^2 + 2{E_{sn}}^2)] \end{aligned} \tag{1}$$

In this study we focus on C_1-α estimation (as they represent the main direction of coupling in the Guccione model [12]) and assume the anisotropy parameters are fixed to the ground truth values (see Section 2.2), following a common approach (see more in [9]). This assumption is revisited in the sensitivity analysis (Section 2.6).

2.2 Generation of synthetic data sets

The left ventricle (LV) was modelled using a truncated prolate spheroidal geometry with human dimensions (bottom left corner in Fig. 1). The constructed finite element (FE) mesh consisted of 320 elements (4 circumferential, 4 transmural, 4 longitudinal and 16 in the apical cap) and 9685 nodes.

The three synthetic cases (SC1, SC2, SC3) were generated by prescribing three variations of basal displacements (shown in top left corner of fig. 1 in green) and passively inflating the reference geometry to different pressure levels (180 Pa for SC1,SC3 and 40 Pa for SC2). The myocyte orientation in the LV was assumed to follow an idealised $-90°/+90°$ distribution from the epi- to the endocardium and the Guccione material model parameters were: $C_1 = 100Pa$, $\alpha = 15$, $r_f = 0.55$, $r_{ft} = 0.25$ and $r_t = 0.2$. The prescribed pressure and the deformed 'LV geometry' (the deformed FE mesh) at each simulation increment represent the pressure-'imaging' data set for each synthetic case.

The deformation was found by solving the linearised total potential energy equations using the *CHeart* nonlinear mechanics solver [7], using a split $\boldsymbol{u}$-p formulation outlined in [4]. The reference ($\boldsymbol{X}$) and deformed geometry ($\boldsymbol{x}$), and local fiber orientation vectors ($\boldsymbol{f}, \boldsymbol{s}, \boldsymbol{n}$) fields were interpolated with cubic-Lagrange shape functions, hydrostatic pressure field (p) interpolation was linear Lagrange. We used *MATLAB* for all pre- and post- processing [1] and *cmGui* for the visualisations [2].

2.3 Estimation of the exponential parameter α from the reformulated energy-based CF

Parameter estimation in this work is based on previous research [9], where unique parameter estimation was achieved with the use of an energy-based cost function (CF), f^{EC}, that allowed determination of the α parameter. This CF used the principle of energy conservation (EC), dictating that the work of internal stresses inside the tissue (W_{int}) stored as elastic energy and the external work of external forces (W_{ext}) are equal, where assumptions of quasi-static loading and absence of residual active tension in the diastolic window of relevance apply. Eq. (3) expresses the external work in terms of the cavity volume (Ω)- cavity pressure p relationship, assuming negligible contribution of epicardial tractions on W_{ext}, as well as that the contribution of basal work on the total external work can be largely accounted for by the increase in cavity volume due to the

[1] https://uk.mathworks.com/products/matlab.html
[2] http://www.cmiss.org/cmgui

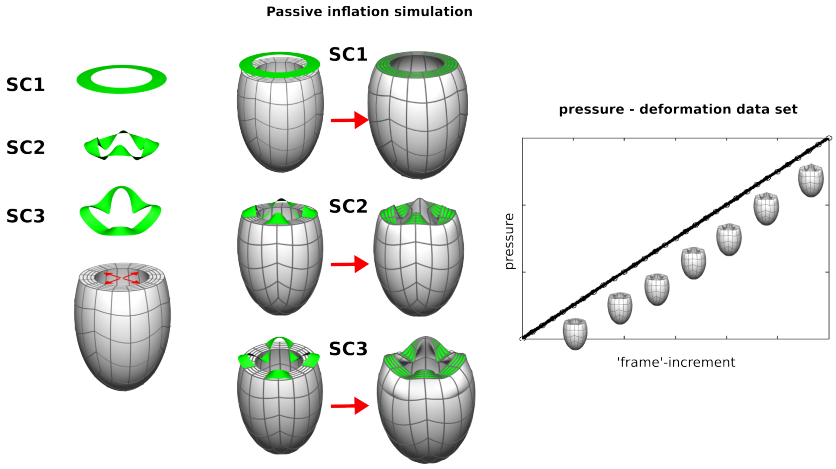

Fig. 1: Generation of the 3 synthetic data sets. A prolate spheroidal mesh representing the left ventricle (LV) was prescribed 3 types of basal displacements and passively inflated to different cavity pressures. SC1 involves a small displacement gradient in the radial direction and none in the circumferential. SC2 is highly varying circumferentially and radially and there is a restriction of zero displacements at the epicardial-basal junction simulating a stiff epicardial rim. SC3 is similar to SC2 but allows for radial expansion. The LV meshes at each simulation increment and the corresponding inflation pressures were treated as LV geometry/pressure data at each 'frame'.

atrioventricular plane motion. In Eqs. (2),(3) Ψ is given by (1), V represents the myocardial domain of the LV and Ω_0, Ω_{def} denote the cavity volume at the reference (unloaded and unstressed) state and deformed state (corresponding to the data frame in question) respectively. Expressing the energy conservation principle over two diastolic frames (DF), DF_1 and DF_2, yielded f^{EC} shown in Eq. (4).

$$W_{int} = \int_V \Psi dV. \tag{2}$$

$$W_{ext} = \int_{\Omega_0}^{\Omega_{def}} p d\Omega \tag{3}$$

$$f^{EC} = \left| \frac{W_{ext}^{DF_1}}{W_{ext}^{DF_2}} - \frac{W_{int}^{DF_1}}{W_{int}^{DF_2}} \right| \tag{4}$$

Instead of energy conservation, the CF employed in this study (f^{VW}) is based on the principle of virtual work (VW), which is a weak expression of the equilibrium. It states the equality of the works of the internal (δW_{int}) and external (δW_{ext}) forces acting on the myocardium along an arbitrary displacement field $\delta \boldsymbol{u}$ called the virtual field. The internal and external components of

the virtual work are given in Eqs. (5) and (6) respectively. Eq. (5) expresses the work of the internal 2^{nd} Piola-Kirchhoff stresses ($\partial\Psi/\partial\boldsymbol{E}$) on the linearised Green-Lagrange strains in the direction of $\delta\boldsymbol{u}$ ($D\boldsymbol{E}[\delta\boldsymbol{u}]$) given in Eqs. (7) and (8). Eq. (6) expresses the work of the cavity pressure p acting on the endocardial boundary along $\delta\boldsymbol{u}$, where d$\boldsymbol{a}$ and $\boldsymbol{F}$ denote the infinitesimal area vector in the deformed configuration and deformation gradient respectively [12, 1]. Expressing the principle of virtual work over 2 diastolic frames DF_1 and DF_2, the modified energy-based CF f^{VW} can then be expressed as in Eq. (9).

Cost functions f^{EC} and f^{VW} allow the unique estimation of α as they are independent of C_1. Clearly since both the numerator and denominator of the ratio of W_{int} or δW_{int} in Eqs. (4) and (9) respectively contain the parameter C_1, it cancels out.

$$\delta W_{int} = \int_V \frac{\partial \Psi}{\partial \boldsymbol{E}} : D\boldsymbol{E}[\delta\boldsymbol{u}]dV. \tag{5}$$

$$\delta W_{ext} = \int_a p d\boldsymbol{a} \cdot \delta\boldsymbol{u} \tag{6}$$

$$\frac{\partial \Psi}{\partial \boldsymbol{E}} = C_1 \alpha \mathrm{e}^Q \begin{bmatrix} r_f & r_{ft} & r_{ft} \\ r_{ft} & r_t & r_t \\ r_{ft} & r_t & r_t \end{bmatrix} \circ \begin{bmatrix} E_{ff} & E_{fs} & E_{fn} \\ E_{sf} & E_{ss} & E_{sn} \\ E_{nf} & E_{ns} & E_{nn} \end{bmatrix} \tag{7}$$

$$D\boldsymbol{E}[\delta\boldsymbol{u}] = \frac{1}{2}\left(D\boldsymbol{F}[\delta\boldsymbol{u}]^T\boldsymbol{F} + \boldsymbol{F}^T D\boldsymbol{F}[\delta\boldsymbol{u}]\right) \tag{8}$$

$$f^{VW} = \left| \frac{\delta W_{ext}^{DF_1}}{\delta W_{ext}^{DF_2}} - \frac{\delta W_{int}^{DF_1}}{\delta W_{int}^{DF_2}} \right| \tag{9}$$

2.4 Estimation of the scaling parameter C_1

Following determination of α from f^{VW} (Section 2.3), parameter C_1 can be estimated from the expression of the principle of virtual work ($\delta W_{ext} = \delta W_{int}$) in one of the two frames DF_1 or DF_2 used in Eq. (9). The estimated value of C_1 using the principle of virtual work and using as input the α parameter from the minimised f^{VW} is denoted by C_1^{VW}. The choice of frame (DF_1 or DF_2) was found to be insignificant with differences in C_1 in the order of 1% and here we present the results for DF_2 for consistency (Eq. (10)). ${C_1}^f$ denotes the assumed C_1 value in Eq. (4),(9) for the estimation of f^{EC}, f^{VW} (in this analysis ${C_1}^f$ was assigned a fixed value of 1 Pa).

For comparison to the previous method based on energy conservation [9] C_1 was also estimated following the α estimation from f^{EC} by expressing the energy balance (W_{ext}=W_{int}) in frame DF_2 - see Eq. (11)- and is denoted by C_1^{EC}.

$${C_1}^{VW} = \frac{\delta W_{ext}^{DF_2}}{\left(\frac{\delta W_{int}^{DF_2}}{{C_1}^f}\right)} \tag{10}$$

$$C_1{}^{EC} = \frac{W_{ext}^{DF_2}}{\left(\frac{W_{int}^{DF_2}}{C_1{}^{f}}\right)} \tag{11}$$

2.5 Generation of virtual field for tackling basal displacements

The virtual field (VF) used in Eq. (5,6) can be any displacement field which conforms with the inherent boundary conditions (BCs) of the problem. In this case the additional restrictions involve respect to incompressibility constraints (in order to overcome the indeterminance of the Lagrange multiplier p from just the deformation data [1]) and zero displacements at the basal boundary so that the unknown boundary tractions due to tissue deformation don't participate in δW_{ext} in Eq. (6). Specifically, the chosen VF was obtained from passively inflating the LV as specified in section 2.2 under a fully fixed base (with Guccione material model parameters: $C_1 = 100$, $\alpha = 15$ and $r_f, r_{ft}, r_t = 1/3$).

2.6 Sensitivity study.

To provide an estimation of the severity of data quality and model-data discrepancies on the estimated parameter values with the VW based approach, a sensitivity study was performed. For estimating effects of miscalibration in pressure measurements, synthetic data sets with modified pressure traces (pressure offset by $\pm 10\%$ of mean pressure value) were used. Additionally data sets with modified deformation fields were examined, were white Gaussian noise with 1 - 10% STD of the mean value was independently applied to the distribution of each of the 9 deformation gradient tensor ($\boldsymbol{F}$) components at the employed Gauss points used for the integration of the energy density function (Eq. (1)). The impact of the assumed fiber field in the model was evaluated by assuming an alternative $-60°/+60°$ fiber angle variation from epi- to endocardium. To investigate the effect of the assumed anisotropy ratio parameter values (r_f, r_{ft}, r_t) alternative assumptions of isotropic ($r_f = 0.34, r_{ft} = 0.33, r_t = 0.33$) or highly anisotropic ($r_f = 0.85, r_{ft} = 0.1, r_t = 0.05$) material assumptions were made in the analysis (see Section 2.3). The results of the sensitivity study are shown in Table 1.

2.7 Basal work contribution quantification at the boundaries

To provide context for the choice of prescribed basal displacements in the 3 synthetic data sets (SC1-3) we estimated the external work at the base (W_{ext}^{base}) with respect to the strain energy (W_{int}) in the myocardium for the ground truth parameters. This ratio was also quantified in 7 clinical data sets from 6 HF patients (PC1,PC3-7, case PC2 was removed as an outlier) and one healthy volunteer (HC) [9]. The estimation of W_{ext}^{base} is given by Eq. (12) [1, 7], where J is the determinant of the deformation gradient $\boldsymbol{F}$. The bottleneck in this estimation is the indeterminate Lagrange multiplier p, which here was provided by

the simulation outputs, but is not available from deformation data. (W_{ext}^{base} estimation in the clinical cases was based on passive inflation simulations with the identified parameters from [9] with cavity pressure and prescribed basal displacements from end diastolic frame 'DF' data). The non-dimensionalised results are shown in Fig 2 in terms of ratios of W_{ext}^{base} with respect to W_{int} in the myocardial domain. Please note that these results provide an 'order of magnitude' level of quantification of the possible contributions of the basal boundary tractions (there are possible numerical errors associated with stress recovery from FE meshes, which have not been accounted for in this work [5]).

$$W_{ext}^{base} = \int_{u=0}^{u_{DF}} \int_{\Gamma_b} [(1/J\boldsymbol{F}\frac{\partial \Psi}{\partial \boldsymbol{E}}\boldsymbol{F}^T - p\boldsymbol{I}) \cdot d\boldsymbol{a}] \cdot \boldsymbol{du} \tag{12}$$

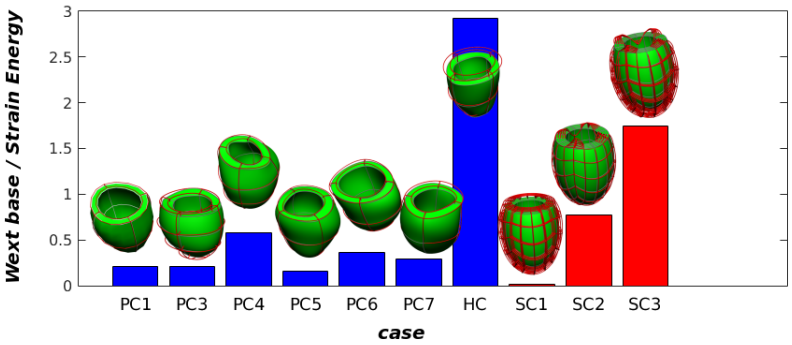

Fig. 2: Comparison of basal work to strain energy ratios at the last 'frame' in the three synthetic data sets (SC1-3) to the ratios of the clinical cases (PC1-7,HC) in [9] at the end diastolic frame (Section 2.7). The reference configuration of each case is shown as green surfaces and the red lines denote the deformed configuration. Note that the highest ratio in the clinical data sets occurs for the healthy case (HC) in accordance with the hypothesis that atrio-ventricular plane displacement is compromised in HF.

3 Results

The results of the parameter estimation study with and without the VW method and the sensitivity analysis for the basal deformation data set SC2 (with the highest offset between identified and ground truth values) are given in Table 1.

4 Discussion

In this work we propose a solution to the presence of unknown basal tractions while still providing a unique myocardial material parameter estimation. The

Table 1: Upper part: Results of parameter estimation with and without use of the modified CF with the virtual fields method in the 3 synthetic data sets (ground truth values: $\alpha = 15$, $C_1 = 100$ Pa). Lower part: Sensitivity analysis results of parameter estimation against data noise and modelling assumptions for the synthetic data set SC2 where the identified parameters varied more from the ground truth (ground truth values: $\alpha = 15$, $C_1 = 100$ Pa). n/a: cost function was unable to identify α parameter (since the estimation of C_1 is derivative, its estimation was also unsuccessful)

Data set / analysis:		f^{EC}		f^{VW}	
Analysis results		α^{EC}	${C_1}^{EC}$ (Pa)	α^{VW}	${C_1}^{VW}$ (Pa)
SC1		15	114	16	108
SC2		n/a	n/a	10	175
SC3		n/a	n/a	16	106
Sensitivity analysis					
Data/Model Modification		α^{EC}	${C_1}^{EC}$ (Pa)	α^{VW}	${C_1}^{VW}$ (Pa)
Default SC2		n/a	n/a	10	175
Pressure	+10% $\bar{p}$ offset	n/a	n/a	9	208
	-10% $\bar{p}$ offset	n/a	n/a	11	147
$\boldsymbol{F}$ noise	STD 1% $\bar{F}_{ij}$	n/a	n/a	9	197
	STD 5% $\bar{F}_{ij}$	n/a	n/a	11	152
	STD 10% $\bar{F}_{ij}$	2	< 0	4	455
Fibers	-/+ 60 ^{o}	n/a	n/a	10	168
r_f-r_{ft}-r_t	0.85-0.1-0.05	n/a	n/a	5	580
	0.34-0.33-0.33	n/a	n/a	11	115

solution is based on an energy-based cost function that overcomes the parameter coupling problem, and the novelty is a modified version of this CF based on the principle of virtual work. Using a virtual field within a weak expression of the equilibrium brings fundamental advantages, since it enables us to render conspicuous aspects of deformation irrelevant to the analysis (i.e. remove the impact of the unknown basal traction). The choice of a suitable virtual field is the core aspect, and prescribing a fixed base in a passive inflation was a relatively simple way of finding it, with easy implementation in clinical data sets. The only simulation required is thus the one that generates the virtual field (a passive inflation of the reference configuration mesh with a fixed base), and the result does no more depend on the accurate estimation of boundary conditions the prediction of deformations.

The feasibility of the method is demonstrated in the analysis of three synthetic data sets (each including cavity pressure and myocardial deformation measurements) generated from a passive inflation simulation with varying degrees of prescribed basal displacements. The virtual work based parameter estimation

(α^{VW}, C_1^{VW}) shows an improved performance in estimating myocardial material parameters in the presence of large basal deformations compared to the original energy based approach (α^{EC}, C_1^{EC}), where there is no valid solution found to the original cost function (f^{EC}) in most of the cases (Table 1). In order to put our results into perspective, it is worth noting that the errors in identified parameters of a 50% are much smaller than the fundamental limitation caused by a non-unique material parameter estimation [8]. Moreover, to provide context for the introduced basal deformations in the synthetic data sets, we first estimated the basal work present in real cases (see Section 2.7). Our situations of basal deformation are thus in the range of observed deformations in clinical data (see Fig. 2). As it may be expected, the clear tendency observed is that the bias is more pronounced in cases with larger deformations (i.e. the healthy case HC), and it has a variable range across the heart failure cases.

The robustness of the method is shown in the sensitivity analysis to basic modelling assumptions and data noise (Table 1). Consistent to original results [9, 8], the factor most compromising accuracy was shown to be the deformation noise, which is modelled in the worst case for the estimation of strain: white noise that has no spatial correlation. Pressure data quality, which is often compromised in clinical data sets, was also shown to be important. On the modelling assumptions side, the least influential factor is the myofiber orientation in the model, but the anisotropy ratios was shown to be critical. a result which comes in antithesis to previous analysis with a $-60°/+60°$ fiber field in the data generating simulation, highlighting the effect of the fixed anisotropy assumption in the presence of a myocardium with very longitudinally oriented fibers at the boundaries.

One last fundamental advantage is that this approach removes the requirement for a complete cavity pressure trace measurement in diastole as the modified CF f^{VW} focuses on two frames only in the diastolic window. Hence only relative pressure measurements are required at these two frames since f^{VW} utilises a pressure ratio only (Eq. 9), unlike the original approach where the cost function f^{EC} requires knowledge of the cavity pressure throughout most of diastole (Eq. 4).

The main limitation of this approach is that it depends more on the quality of the data, in this case of the deformation field that is used to estimate the strain energy. Cost functions can be defined in terms of much more robust observations, such as volume, but at the cost of lack of identifiability of estimated parameters. Image analysis techniques that extract deformation fields that respect model assumptions [2] can provide a solution to alleviate this dependence. Moreover, the proposed parameter estimation procedure relies on a single 'frame' combination (DF_1,DF_2) for α and on DF_2 only for C_1 based on our results that indicated frame independent in silico. However this step will need to be revised before application of the method to clinical data sets and more frames will need to be incorporated in the pipeline in anticipation of data noise.

Future extensions of this work involve exploration of the application of the virtual fields method to eliminate the effect of external tractions in the remain-

ing boundaries of the ventricle (i.e. the impact of the right ventricle and the kinematic constraints on the epicardium) and its translation to clinical data sets.

5 Acknowledgements

This work was supported by the Wellcome/EPSRC Centre for Medical Engineering [WT 203148/Z/16/Z] and by the National Institute for Health Research (NIHR) Cardiovascular MedTech Co-operative. PL holds a Wellcome Trust Senior Research Fellowship [209450/Z/17/Z].

References

1. Bonet, J., Wood, R.D.: Nonlinear Continuum Mechanics for Finite Element Analysis. Cambridge University Press, second edn. (2008)
2. Genet, M., Stoeck, C., von Deuster, C., Lee, L., Kozerke, S.: Equilibrated warping: Finite element image registration with finite strain equilibrium gap regularization. Medical Image Analysis 50, 1 – 22 (2018)
3. Guccione, J.M., McCulloch, A.D., Waldman, L.K.: Passive material properties of intact ventricular myocardium determined from a cylindrical model. Journal of biomechanical engineering 113(1), 42–55 (mar 1991)
4. Hadjicharalambous, M., Lee, J., Smith, N.P., Nordsletten, D.A.: A displacement-based finite element formulation for incompressible and nearly-incompressible cardiac mechanics. Comput Methods Appl Mech Eng 274(100), 213–236 (jun 2014)
5. Kasper, E.P., Taylor, R.L.: A mixed-enhanced strain method: Part i: Geometrically linear problems. Computers and Structures 75(3), 237 – 250 (2000)
6. Lamata, P., Casero, R., Carapella, V., Niederer, S.A., Bishop, M.J., Schneider, J.E., Kohl, P., Grau, V.: Images as drivers of progress in cardiac computational modelling. Progress in biophysics and molecular biology 115(2-3), 198–212 (aug 2014)
7. Lee, J., Cookson, A., Roy, I., Kerfoot, E., Asner, L., Vigueras, G., Sochi, T., Deparis, S., Michler, C., Smith, N.P., Nordsletten, D.A.: Multiphysics Computational Modeling in CHeart. SIAM J Sci Comput 38(3), C150–78 (may 2016)
8. Nasopoulou, A., Nordsletten, D.A., Niederer, S.A., Lamata, P.: Feasibility of the estimation of myocardial stiffness with reduced 2d deformation data. In: Pop, M., Wright, G.A. (eds.) Functional Imaging and Modelling of the Heart. pp. 357–368. Springer International Publishing, Cham (2017)
9. Nasopoulou, A., Shetty, A., Lee, J., Nordsletten, D., Rinaldi, C.A., Lamata, P., Niederer, S.: Improved identifiability of myocardial material parameters by an energy-based cost function. Biomechanics and Modeling in Mechanobiology 16(3), 971–988 (Jun 2017)
10. Palit, A., Franciosa, P., Bhudia, S.K., Arvanitis, T.N., Turley, G.A., Williams, M.A.: Passive diastolic modelling of human ventricles: Effects of base movement and geometrical heterogeneity. Journal of Biomechanics 52, 95 – 105 (2017)
11. Westermann, D., Kasner, M., Steendijk, P., Spillmann, F., Riad, A., Weitmann, K., Hoffmann, W., Poller, W., Pauschinger, M., Schultheiss, H.P., Tschöpe, C.: Role of left ventricular stiffness in heart failure with normal ejection fraction. Circulation 117(16), 2051–60 (apr 2008)

12. Xi, J., Lamata, P., Niederer, S., Land, S., Shi, W., Zhuang, X., Ourselin, S., Duckett, S.G., Shetty, A.K., Rinaldi, C.A., Rueckert, D., Razavi, R., Smith, N.P.: The estimation of patient-specific cardiac diastolic functions from clinical measurements. Med Image Anal 17(2), 133–46 (feb 2013)